EPS-HEP 95 Ref. eps0570
Submitted to Pa 1, 8, 14, 15
Pl 4, 11, 18, 19

DELPHI 95-89 PHYS 524
30 June, 1995

# Measurement of the partial decay width $R_b = \Gamma_{b\bar{b}}/\Gamma_{had}$ with the DELPHI detector at LEP

DELPHI Collaboration

Paper submitted to the "EPS-HEP 95" Conference
Brussels, 27th July-2nd August 1995

EPS-HEP 95 Ref. eps0570
Submitted to Pa 1, 8, 14, 15
Pl 4, 11, 18, 19

DELPHI 95-89 PHYS 524
30 June, 1995

# Measurement of the partial decay width $R_b = \Gamma_{b\bar{b}}/\Gamma_{had}$ with the DELPHI detector at LEP

Preliminary

DELPHI Collaboration

P. Billoir, G. Borisov, E. Cortina, E.Higon, M. Margoni, C. Mariotti, F. Martinez-Vidal, K. Moenig, P. Ronchese, J.Salt, F. Simonetto, Ch. de la Vaissiere

**Abstract**

The partial decay width of the $Z$ to $b\bar{b}$ quark pairs has been measured by the DELPHI detector at LEP. $b$-hadrons, containing $b$-quarks, were tagged by several methods using leptons with high transverse momentum relative to the hadron or by tracks with large impact parameters to the primary vertex sometimes complemented by event shape variables.

The ratio of the numbers of events with a single such tag to those with two tags was used to estimate the efficiency of the method and to reduce the systematic uncertainty. Combining all methods, the value:

$$\frac{\Gamma_{b\bar{b}}}{\Gamma_{had}} = 0.2210 \pm 0.0016(stat) \pm 0.0020(syst) \pm 0.0012(\Gamma_{c\bar{c}})$$

was found, where the third error corresponds to a $\pm 8\%$ variation of the $c\bar{c}$ production fraction around its standard model value.

# 1 Introduction

A precise measurement of the relative decay width of the $Z$ into $b$-hadrons, $R_b = \frac{\Gamma_{b\bar{b}}}{\Gamma_{had}}$, is an important test of the Standard Model which predicts a value that is dependent on the top mass $m_t$ [1] via weak vertex corrections. To a large extent the ratio is independent of other corrections such as QED or QCD corrections or electroweak corrections to the $Z$-propagator.

This paper presents three measurements of $R_b$[1] using data taken until 1993 with the DELPHI detector at LEP. In a first analysis b quark hemispheres are tagged by the presence of large impact parameter tracks. Comparing single and double tag rates $R_b$ can be measured together with the b-tagging efficiency. A second analysis uses the same tagging method as the first one. However the tagging efficiency is measured from hemispheres opposite to a high $p_t$ lepton. $R_b$ can then be measured from the single tag rate. The statistical precision is determined by the events having two tags. For that reason the statistical correlation between the two methods is small. Also the systematic uncertainties are largely different. Since the tagging method is rather simple the tagging efficiency for light and c quark events can be estimated reliably from simulation. Contrary to that the third analysis uses a sophisticated tagging method combining thirteen vertex and event shape variables in a multivariate approach. All efficiencies are estimated from data using a complex $\chi^2$ fit. The two first analyses are updated using 1993 data (1991 and 1992 results have been shown at previous conferences [2] and have been published recently [3]) meanwhile the third one uses the 1992 and 1993 data and updates the 1991 result [4]. The three analyses are combined taking into account all correlations.

# 2 The DELPHI Detector

The DELPHI detector has been described in detail in ref. [5]. Only the details most relevant to this analysis are mentioned here.

In the barrel region, the charged particle tracks are measured by a set of cylindrical tracking detectors whose axes are parallel to the 1.2 T solenoidal magnetic field and to the beam direction. The time projection chamber (TPC) is the main tracking device. The TPC is a cylinder with a length of 3 m, an inner radius of 30 cm and an outer radius of 122 cm. Between polar angles, $\theta$, of 39° and 141° with respect to the beam direction, tracks are reconstructed using up to 16 space points. Outside this region (21° to 39° and 141° to 159°), tracks can be reconstructed using at least 4 space points.

Additional precise $R\Phi$ measurements, in the plane perpendicular to the magnetic field, are provided at larger and smaller radii by the Outer and Inner detectors respectively. The Outer Detector (OD) has five layers of drift cells at radii between 198 and 206 cm and covers polar angles from 42° to 138°. The Inner Detector (ID) is a cylindrical drift chamber having inner radius of 12 cm and outer radius of 28 cm. It covers polar angles between 29° and 151°. It contains a jet chamber section providing 24 $R\Phi$ coordinates surrounded by five layers of proportional chambers providing both $R\Phi$ and longitudinal $z$ coordinates.

The micro-vertex detector (VD) is located between the LEP beam pipe and the ID [6].

[1]The numbers presented in this note always correspond to the ratio of cross sections $\sigma(e^+e^- \to b\bar{b})/\sigma(e^+e^- \to hadrons)$. To obtain the ratio of partial widths 0.0003 has to be added to the numbers.

It consists of three concentric layers of silicon microstrip detectors placed at radii of 6.3, 9 and 11 cm from the interaction region. For all layers the microstrip detectors provide hits in the $R\Phi$-plane with a measured intrinsic resolution of about 8 $\mu$m. The polar angle coverage for charged particles hitting all three layers of the detector is 42.5° to 137.5°.

The barrel electromagnetic calorimeter, HPC, covers the polar angles between 42° and 138°. It is a gas-sampling device which provides complete three dimensional charge information in the same way as a time projection chamber. Each shower is sampled nine times in its longitudinal development. Along the drift direction, parallel to the DELPHI magnetic field, the shower is sampled every 3.5 mm ; in the plane perpendicular to the drift the charge is collected by cathode pads of variable size, ranging from 2.3 cm in the inner part of the detector to 7 cm in the outer layers. The excellent granularity allows good separation between close particles in three dimensions and hence good electron identification even inside jets.

Muon identification in the barrel region is based on a set of muon chambers (MUB), covering polar angles between 53° and 127°. It consists of six active planes of drift chambers, two inside the return yoke of the magnet after 90 cm of iron (inner layer) and four outside after a further 20 cm of iron (outer and peripheral layers). The inner and outer modules have similar azimuthal coverage. The gaps in azimuth between adjacent modules are covered by the peripheral modules. Therefore a muon traverses typically either two inner layer chambers and two outer layer chambers, or just two peripheral layer chambers. Each chamber measures the $R\Phi$ coordinate to 2–3 mm. Measuring $R\Phi$ in both the inner layer and the outer or peripheral layer determines the azimuthal angle of muon candidates leaving the return yoke within about $\pm 1°$. These errors are much smaller than the effects of multiple scattering on muons traversing the iron.

# 3 Event Selection

The criteria to select charged tracks and to identify hadronic Z decays have been identical to those described in [3].

About 700000 hadronic $Z$ decays have been selected from the 1993 data sample where the exact numbers vary slightly between the different analyses due to different requirements on the detector availability. A sample about twice the data statistics of $Z \to q\bar{q}$ events has been simulated using the Lund parton shower Monte Carlo JETSET 7.3 [7] with parameters optimized by DELPHI and the DELPHI detector simulation [8]. In addition dedicated samples of $Z \to b\bar{b}$ events have been generated. The simulated events have been passed through the same analysis chain as the real ones.

# 4 The Lifetime Analysis

The method used for this measurement of $R_b$ is nearly identical to the one described in [3]. In the following only the features different from the 1992 analysis will be described in detail. Since for the measurement of impact parameters the VD is essential the method is limited to events with most tracks inside the VD acceptance. For this reason a cut on $|\cos\theta_{thrust}| < 0.65$ is applied. This cut is harder than the one applied in [3], because in 1993 due to some inconsistency in the VD position between data and simulation the description of the edge of the VD acceptance was slightly inaccurate.

| Source of systematics | $\Delta\epsilon_{uds} \times 10^4$ |
|---|---|
| MC statistics | $\pm 0.5$ |
| Detector resolution | $\pm 0.8$ |
| $K^0$ | $\pm 0.4$ |
| Hyperons | $\pm 0.1$ |
| Photon conversions | $\pm 0.1$ |
| Gluon splitting $g \to b\bar{b}$ | $\pm 0.7$ |
| Gluon splitting $g \to c\bar{c}$ | $\pm 0.3$ |
| Total | $\pm 1.3$ |

Table 1: Systematic errors of light quark efficiency $\epsilon_{uds}$.

Since for this analysis a good description of the data by the simulation is required, some tuning of the impact parameter distribution in the simulation has to be done. This procedure has been refined with respect to the 1992 analysis basically by taking into account small inhomogeneities in the azimuthal angle. This leads to substantially smaller uncertainties due to the understanding of the detector resolution.

## 4.1 Estimates of Efficiencies and Correlations

The analysis was performed at many different cut values and combined with the 1991/1992 number. The total error has been found to be almost constant between cuts of $-\log_{10}(P_H) > 2.7$ and $-\log_{10}(P_H) > 2.9$. To decrease the correlation of this analysis with other ones the hardest of these cut has been chosen for the final numbers.

The values of the light quark efficiencies ($\epsilon_c$, $\epsilon_{uds}$), and the hemisphere correlation ($\rho_b$) with this cut were extracted from the simulation and the possible sources of uncertainties were included as systematic errors.

The value of $\epsilon_{uds}$ was found to be:

$$\epsilon_{uds} = (0.252 \pm 0.013) \times 10^{-2}. \tag{1}$$

The different sources of systematics are given in the Table 1.

The systematic error coming from the differences in resolution between data and simulation was estimated as the difference of the tagging efficiencies in data and in simulation when hemisphere probabilities were computed using tracks with negative impact parameters ("negative hemisphere probability").

The systematic error from the uncertainties in production of long lived particles in light quark events ($K^0$, $\Lambda$, hyperons) was obtained by varying the corresponding production rates in simulation by $\pm 10\%$. This variation corresponds to the observed differences between the production rate of these particles in data and simulation and agrees with the recommendations of [9]. The systematics from the gluon splitting $g \to b\bar{b}$ and $g \to c\bar{c}$ were obtained by varying the fraction of such events by $\pm 50\%$ [9]. In addition to these systematic sources, it was checked that the uncertainties from the interactions of particles in the material of the detector are negligible.

The efficiency to tag hemispheres with charm was found to be:

$$\epsilon_c = (1.60 \pm 0.14) \times 10^{-2} \tag{2}$$

| Source of systematics | $\Delta\epsilon_c \times 10^4$ |
|---|---|
| MC statistics | $\pm 2.0$ |
| Detector resolution | $\pm 4.0$ |
| Production rates of charm hadrons | $\pm 10.6$ |
| Charged decay multiplicities | $\pm 3.8$ |
| $D \to K^0 X$ | $\pm 6.6$ |
| Charmed hadrons lifetime | $\pm 2.7$ |
| Fragmentation | $\pm 3.0$ |
| Total | $\pm 14.0$ |

Table 2: Systematic errors of charm quark efficiency $\epsilon_c$

The simulation has been tuned to describe as well as possible the properties of charm production and decays as measured at LEP and at lower energies. For the evaluation of the systematic uncertainty the following parameters have been varied within their measurement error:

- the production ratios of the different charmed hadrons [9],
- the charged decay multiplicities of charmed hadrons [10],
- the inclusive branching ratios $D \to K^0 X$ [11],
- the $c$-hadron lifetimes [11],
- the mean energy of $c$-hadrons in fragmentation as suggested in [9].

For the central values and the errors we follow the prescription of [9]. The sources of systematic error are listed in table 2.

For the light quark efficiency mostly the accurate description of the resolution function in the probability calculation is important, assuring a flat distribution of the hemisphere probability. On the contrary, for charm the agreement between data and simulation is relevant, since tracks from charm decays have real impact parameters. An estimate of the uncertainty due to the knowledge of the detector resolution was obtained from the change in $\epsilon_c$ assuming the resolution curve obtained from the data in the calculation of the probabilities in the simulation. Since the error assignment to the impact parameters is the same in data and simulation the difference in the resolution curve reflects the difference in the true resolution.

The correlation between hemispheres in $b$ events was evaluated to be

$$\rho_b = (-1.28 \pm 0.13(stat) \pm 0.09(syst)) \times 10^{-2}. \tag{3}$$

The correlation can be described mainly in terms of four sources:

- radiation of hard gluons: This source acts in two ways. Due to gluon radiation, energy is taken away from the $b$-hadrons. Since the resolution is largely determined by the multiple scattering in the beam pipe this lowers the tagging efficiency. This leads to a positive correlation. In about 2% of the cases both $b$-hadrons are boosted into the same hemisphere, leading to a negative correlation.

- the polar angle of the thrust axis: Since both jets either are in a region of good or somewhat worse VD acceptance this leads to a positive correlation.
- the azimuthal angle of the jets: Due to dead or noisy modules in the vertex detector the efficiency was not completely flat in $\Phi$. However in the data sample presented here most modules have been highly efficient.
- the bias of the fitted production vertex due to the inclusion of tracks from $b$ decays, leading to a negative correlation. The effect can be described best by the dependence of the correlation on the B lifetime.

Figure 1 shows the total correlation as a function of the cut value, together with each of these four components and their sum. In the region that is used for the analysis the total correlation is well described by the sum of the components described above.

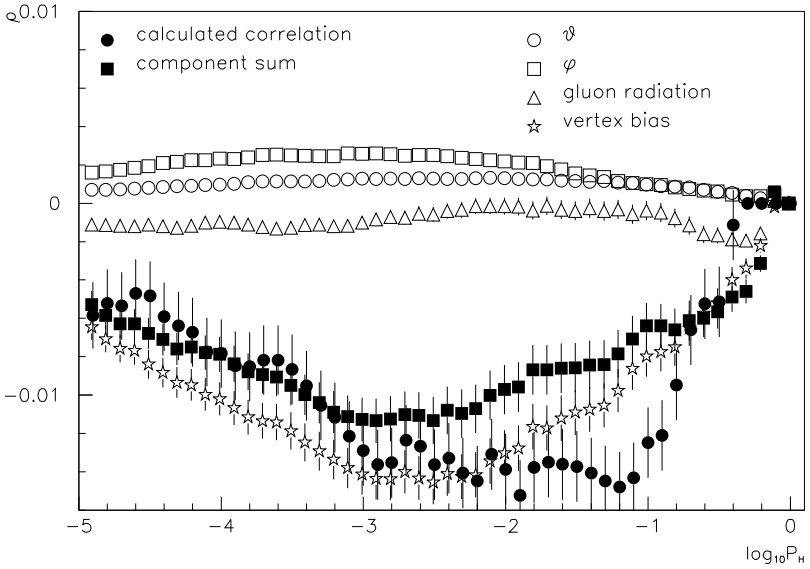


Figure 1: Total hemisphere correlation and individual contributions as a function of the cut value $\log_{10} P_H$.

To obtain the systematic error of the correlation estimate in the simulation the fraction of tagged events was measured in data and in simulation using all events as a function of the relevant variable. From this the correlation due to the single variable considered was calculated. The result was scaled by the ratio of the correlations in $b\bar{b}$ and in all events obtained from the simulation. As the error estimate, the larger of either the difference between the data and simulation measurement or the error of this difference was taken. In the case of gluon radiation thrust was used as testing variable. To account for the cancelation of the two different effects thrust was signed in each hemisphere to be positive for the hemisphere with the larger invariant mass and negative in the other one.

To estimate the description of the correlation due to the vertex bias for each event two hemisphere vertices have been fitted including the beamspot and using only the tracks that have been used for the primary vertex fit. The correlation has been calculated as function of the distance between the hemisphere and the event vertex. The distance has been signed positive if the hemisphere considered is pulling the vertex more than the opposite one if the beamspot is not included in the fit and negative otherwise.

Since this distance is by itself already an efficient b-tagging variable the obtained correlation for the vertex bias is strongly effected by the presence of light quark event. For this reason a hemisphere was only used to measure the vertex bias correlation if the other hemisphere was tagged as a b hemisphere. The extracted correlation for data and MC is shown in figure 2 for data and Simulation.

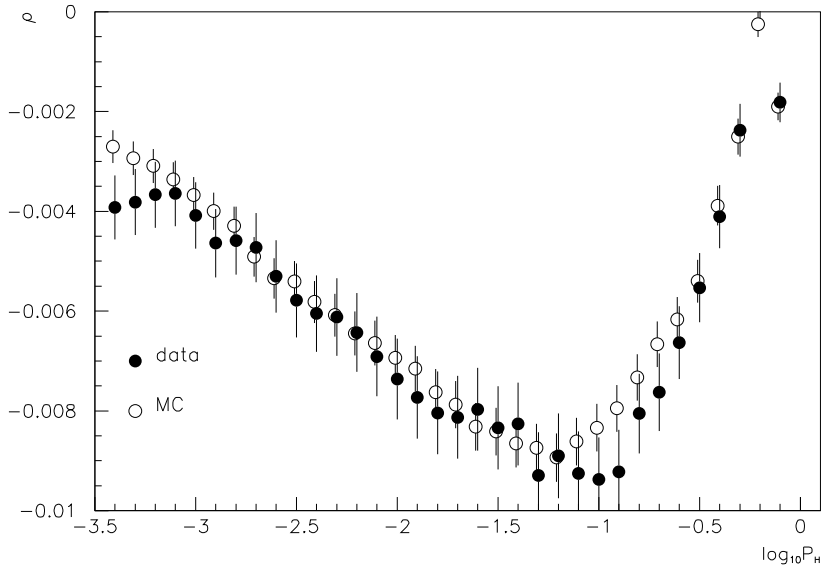


Figure 2: Hemisphere correlation due to vertex bias. The close and open points show the values obtained with the procedure described above for data and simulation.

The different sources of the systematic errors are listed in the table 3.

## 4.2 Results

Using the above values of efficiencies and correlation with their errors the measured value of $R_b$ is equal to:

$$R_b = 0.2215 \pm 0.0027(stat) \pm 0.0029(syst) \pm 0.0018(R_c). \quad (4)$$

For this number $R_c$ was assumed to have its standard model value (0.171) with an 8% relative uncertainty. The $b$ hemisphere tagging efficiency was found to be $\epsilon_b = 0.211 \pm 0.003$ compared to $\epsilon_b(MC) = 0.209$ obtained from the simulation. The breakdown of the error for the given cut on $P_H$ is given in table 4.

| Source of systematics | $\Delta\rho_b \times 10^4$ |
|---|---|
| Resolution function | $\pm 1.0$ |
| Polar angle acceptance | $\pm 2.2$ |
| Azimuthal angle acceptance | $\pm 3.9$ |
| Hard gluon emission | $\pm 6.3$ |
| Lifetime of $b$-hadrons | $\pm 4.8$ |
| total | $\pm 9.2$ |

Table 3: Systematic errors of correlation factor $\rho_b$.

| Error Source | $\Delta R_b \times 10^3$ |
|---|---|
| Statistical error | $\pm 2.7$ |
| Light quark efficiency | $\pm 0.8$ |
| Charm efficiency | $\pm 2.3$ |
| Correlation | $\pm 1.5$ |
| $\Gamma_{c\bar{c}}$ | $\pm 1.8$ |
| Total | $\pm 4.3$ |

Table 4: Sources of errors for measurement of $R_b = \Gamma_{b\bar{b}}/\Gamma_{had}$.

As a cross-check of this measurement, the comparison of $R_b$ values for different tagging cuts is given in Fig. 3. The measured value of $R_b$ is stable over a wide range of variation of the efficiencies and correlation.

## 4.3 Combination with the 91/92 Analysis

In order to combine the analysis presented here with a similar one made with the published one [3], the following assumptions have been made:

- All statistical errors are assumed to be independent.
- The errors in the hemisphere correlations due to hard gluon emission and polar angle acceptance are assumed to be fully correlated between the two years. The uncertainty due to the vertex bias is strongly connected with the uncertainty in the b-hadron lifetime. For this reason the vertex bias error of this analysis has been assumed to be fully correlated with the error labeled "b-hadron lifetime" in [3]. The error due to azimuthal dependence has been assumed uncorrelated since it arises mainly due to dead VD modules which are repaired year by year.
- The tuning of the resolution function in the simulation is done year by year comparing the simulation with the data. Thus the errors due to resolution functions have been assumed to be independent.
- The errors due to the modeling of the light and charm quarks was assumed to be fully correlated.

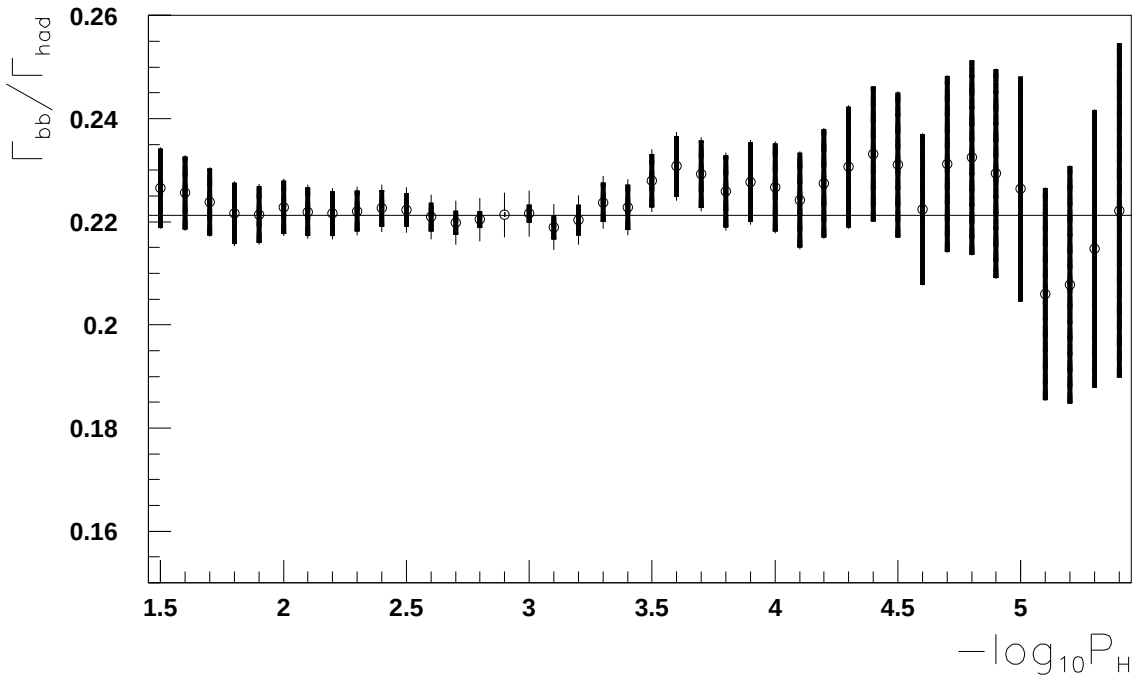


Figure 3: The value of $\Gamma_{b\bar{b}}\ /\Gamma_{had}$ with its total error as a function of the cut on $-\log_{10} P_H$. The straight line corresponds to the value measured at $-\log_{10} P_H > 2.9$. The thin error bar corresponds to the total error, the thick one indicates the part that is independent from the reference point.

With these assumptions the result for the combined data is:

$$R_b = 0.2216 \pm 0.0017(stat) \pm 0.0027(syst) \pm 0.0018(R_c) \tag{5}$$

The breakdown of the error is given in table 10.

## 4.4 Energy dependence

In 1993 data have been taken at three different center of mass energies ($\sqrt{s} = 89.49, 91.25, 93.08 GeV$). Since photon exchange and $\gamma - Z-$ interference are strongly suppressed at energies close to the Z resonance, $R_b(\sqrt{s}) = \frac{\sigma(e^+e^- \to b\bar{b})}{\sigma(e^+e^- \to hadrons)}$ is predicted to be about constant within the Standard Model. However if $R_b$ is affected by the interference of the $Z$ with a $Z'$ almost degenerate in mass as recently suggested by Caravaglios and Ross [12] some energy dependence can be expected. Since the b tagging efficiency varies only very little within the energy range considered here no complicated single to double tag comparison is needed to measure $\frac{R_b(\sqrt{s})}{R_b(91.25GeV}$. Instead simply the ratio of the fraction of tagged events is used with small corrections due to the b tagging efficiency and almost negligible corrections due to background. The measurement has been done using the event probability instead of hemisphere probabilities. The measurement has been performed at several different values of the event probability cut where a minimum statistical error has been found at $\log_{10} P_E > -1.6$. At this value of the cut the b-tagging efficiency varied by a relative amount of $\pm 0.5\%$ with respect to the Z peak and was about

70%, the efficiency to tag c (uds) events was about 20 (4) %. To avoid systematic uncertainties due to time dependence of the b-tagging efficiency the data taken in the first part of the year, where LEP ran only at the Z peak, have been neglected. With these requirements the following ratios have been found:

$$\frac{R_b(89.49GeV)}{R_b(91.25GeV)} = 0.982 \pm 0.015$$
$$\frac{R_b(93.08GeV)}{R_b(91.25GeV)} = 0.997 \pm 0.016$$

The error is statistical only including the limited Monte Carlo statistics at the off peak points. All systematic uncertainties have been found to be negligible. The standard model predicts a ratio of 0.997 (0.998) for the point below (above) the peak with respect to the peak. Figure 4 shows the stability of the measurement with respect to the cut value.

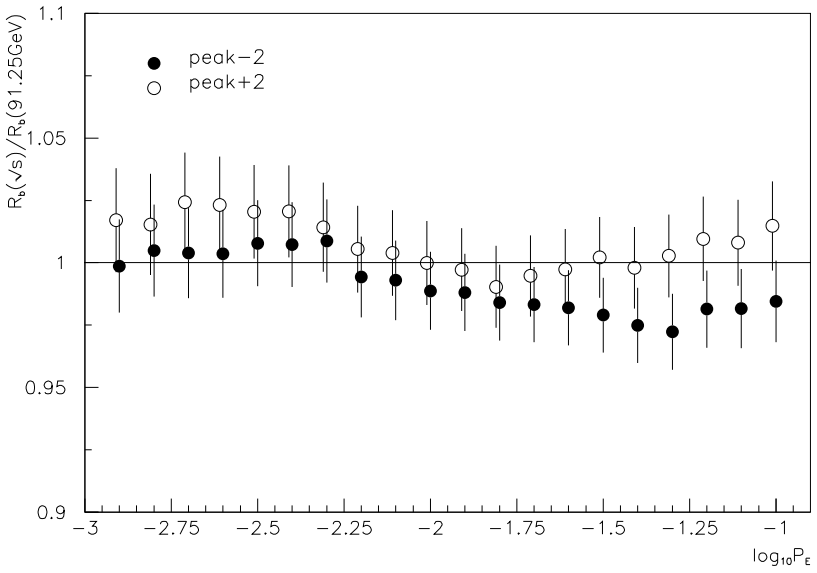


Figure 4: Ratio of the $R_b$ values off-peak with respect to the peak as a function of the cut value.

# 5 Mixed tag Analysis

In this analysis the lifetime $b$ tagging technique described in section 4 was used. The efficiency of the tag was however measured in a sample of events enriched in $b$ semi-leptonic decays. The means of the lepton identification are described in ref. [3]. To increase the fraction of events from $b$ in the sample a cut was applied to the transverse momentum of the lepton with respect to the jet axis after removal of the lepton itself. A cut of $p_t^{out} > 1.5GeV/c$ was used in this analysis. Be $\epsilon_q$ the probability of tagging one

hemisphere by means of this selection when a $q$ ($q = b$,$c$,$uds$) flavour is produced in the $Z$ decay, and $P_q, (q = b, c, uds)$ the fraction of events from the flavour $q$ ($=b, c, uds$) in the lepton subsample. The following set of equations holds:

$$\begin{cases} f_1 &= \epsilon_b R_b + \epsilon_c R_c + \epsilon_{uds} R_{uds} \\ f_2 &= c_l^b \epsilon_b P_b + c_l^c \epsilon_c P_c + c_l^{uds} \epsilon_{uds} P_{uds} \end{cases} \tag{6}$$

where $f_1$ is the fraction of hemispheres in hadronic $Z$ events tagged by the lifetime selection and $f_2$ is the fraction of semileptonic decays tagged by the same selection in the hemisphere opposite to the lepton. To extract with adequate precision the efficiency of the lifetime tags, the accurate knowledge of the flavour composition of the lepton sample, as expressed by the coefficients $P_q, (q = b, c, uds)$, is required. Section 5.1 is devoted to this topic.

The coefficients $c_l^q$ account for correlations between lifetime and lepton tags in opposite hemispheres and were computed by simulation. Due to the small amount of contamination from $c$ and light quarks, only the knowledge of $c_l^b$ was relevant for the measurement.

With the requirement $P_H < 4 \times 10^{-3}$, the efficiency of the $c$ and $uds$ tagging and the coefficient $c_l^b$ were estimated in the simulation as:

$$\begin{aligned} \epsilon_{uds} &= (0.71 \pm 0.01)\% \\ \epsilon_c &= (3.67 \pm 0.04)\% \\ c_l^b &= 1.014 \pm 0.008 \pm 0.005 \end{aligned}$$

The systematic uncertainty on the coefficient $c_l^b$ was determined in the same way as for the lifetime analysis correlation.

With the same probability cut 2891 events were selected, out of 11204 having the high $p_t$ lepton, and a value:

$$R_b = 0.2238 \pm 0.0039$$

was derived, where the error is only statistical. As the cut on the lepton $p_t^{out}$ is an arbitrary parameter, chosen so as to minimize the total error, the variation of the $R_b$ value when changing the $p_t^{out}$ selection was checked. Figure 5 shows the results of this test, where the measured $R_b$ value is reported for different independent $p_t^{out}$ ranges.

The systematic errors will be discussed in section 5.2.

## 5.1 The Composition of the Lepton Sample

The results of the fit to the single and di-lepton distributions (performed on the 1993 data sample by the same means as discussed in ref. [3] ) allowed a precise determination of the fraction $P_b$ ($P_c$) of events from $b$ ($c$) quarks in the lepton sample. The lepton purities were computed in the subset of hadronic events selected for the vertex analysis as a function of $p_t$. The most energetic candidate was used when more than one lepton was found in the event (due to the high $p_t$ cut, this applied to less than 1 % of the cases). The requirement $p_t^{out} > 1.5\text{GeV}/c$ was applied in order to minimize the overall error on $R_b$. The data sample consisted then of 11204 events. The purities of the sample were estimated as:

$$P_b = (81.17 \pm 0.79)\%$$

$$P_c = (9.56 \pm 0.76)\%.$$

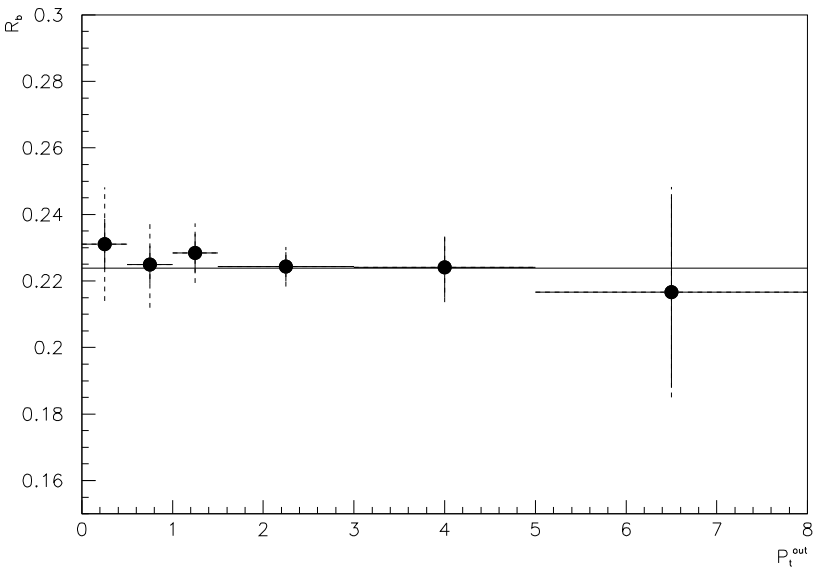


Figure 5: $R_b$ versus the transverse momentum of the lepton. The bins are uncorrelated. The statistical errors are marked. The continuous line shows the result quoted in the text, obtained with the cut $p_t^{out} > 1.5\text{GeV}/c$.

Table 5 shows the individual effect of all the considered error sources on $P_b$. $P_c$ is affected by the same sources of uncertainties as $P_b$, but the biggest contribution to its error is induced by the uncertainties on the amount of the hadron background in the lepton sample

| Source | $\Delta P_b$ |
|---|---|
| Monte Carlo statistics | 0.31 |
| Lepton Fit | 0.36 |
| Model $b \to l$ | 0.39 |
| Model $c \to l$ | 0.31 |
| $b \to \tau \to l$ | 0.03 |
| $b \to \overline{c} \to l$ | 0.02 |
| $b \to J/\Psi \to l$ | 0.03 |
| $c \to l$ | 0.34 |
| $e$ misidentification | 0.12 |
| $\mu$ misidentification | 0.14 |
| $e$ identification efficiency | 0.02 |
| $\mu$ identification efficiency | 0.04 |

Table 5: Systematic errors (%) on the purity of the lepton sample, when the selection $p_t^{out} > 1.5\text{GeV}/c$ was applied to the lepton transverse momentum.

## 5.2 Systematic Errors

Basically three sources of systematic errors have to be considered for the mixed tag $R_b$ measurement:

a) uncertainties coming from the light quark efficiencies,

b) uncertainties coming from correlation effects,

c) uncertainties coming from the knowledge of the composition of the lepton sample.

Errors from sources a) and b) have been evaluated exactly in the same way as in section 4. The effect of the unknowns on the light quark efficiencies turn out to be about a factor two smaller, since they enter only linearly in the equations determining $R_b$.

The error on the correlation between the lepton tag and the vertex tag is dominated by the limited statistics from simulation available. The two most relevant sources of correlation were the gluon radiation and the acceptance of the involved detectors. In fact, the hole between the barrel and forward muon chambers corresponds to a $\cos\theta$ region were the VD sensitivity is reduced; in the same way the HPC polar acceptance overlaps with that of the micro-vertex detector (see section 2). As a consequence of this, when a jet happened to fall near the border of the sensitive region of the micro-vertex detector, the chance to miss the lepton in the opposite hemisphere was higher. This induced positive correlation between the two tags.

The contributions due to the uncertainties in the purity of the lepton sample were then added to the total error. The value of $R_c$ was varied by 8% around its standard model value. Table 6 gives the detailed contributions of all the sources of uncertainty considered above.

| Source of error | $\delta R_b$ |
|---|---|
| statistical | 0.0039 |
| $P_b$ | 0.0024 |
| $P_c$ | 0.0003 |
| Resolution Function | 0.0011 |
| vertex-lepton correlations | 0.0022 |
| $R_c$ | 0.0012 |
| charm efficiency | 0.0018 |
| uds efficiency | 0.0006 |
| total | 0.0057 |

Table 6: Contributions to the total error.

## 5.3 Combination with the 92 Analysis

In order to combine the results of this analysis with the 1992 one ([3]), we treated as independent all the statistical uncertainties.

For the combination of systematic errors we assumed:

- The uncertainty on the correlation between the two selections due to gluon radiation and detector acceptances was considered to be fully correlated.
- The errors on the resolution functions were assumed to be independent, as for the lifetime analysis; the other uncertainties on the charm and light quarks efficiencies were treated as fully correlated.

- The errors on the lepton purity due to Monte Carlo statistics were assumed to be independent, while we treated as fully correlated the uncertainties due to the heavy flavours decay models and Branching Ratios, as the errors due to the lepton efficiencies and the background estimation.

With these assumptions for the 1992/93 data, we obtained:

$$R_b = 0.2231 \pm 0.0029(stat) \pm 0.0035(syst) \pm 0.0012(R_c) \quad (7)$$

# 6 The Multivariate Analysis

The measurement presented in this section uses about 1400000 hadronic $Z$ decays taken in 1992/1993 using the method presented in [13] and already applied for the analysis of the 1991 data taken [4]. The analysis is described in detail in [14]. The cut $\mid cos\theta_{thrust} \mid < 0.75$ was made on the cosine of the polar angle of the thrust axis. This insured that most of the tracks were within the acceptance of the microvertex detector. Two simulated samples of 1.2M/1.5M events were used. In order to improve the independence between opposite hemispheres, a primary vertex was computed on each side using as a constraint the beam spot position and dimensions.

The tagging algorithm combines thirteen microvertex and event shape variables and it is based on an involved multivariate analysis technique. The details of the technique and the description of variables can be found in [13, 14].

The distribution of the classification criteria (called winning margin $\Delta$), played a critical role in the classification of events into categories. It depended significantly on the response of the tracking system so that imperfect simulations of the detector accuracy produced disagreement between data and Monte Carlo. With this analysis, the effect of imperfect simulation of the detector was expected to be small because the efficiencies and backgrounds were estimated directly from the data. A precise study of systematic effects required, however, a rather close agreement between data and simulation. In order to improve this agreement, the winning margin in the simulated sample was corrected in such a way that the distribution in each tag coincided with that of the data sample[2]. Figure 6 shows the winning margin distribution in the $b$ tag after this weighting. This procedure improved the agreement in the description of the detector response. As explained in section 6.3, the difference between the measured $R_b$ using the standard and the corrected simulation was taken as a systematic error coming from the imperfections in the simulation of the detector response.

## 6.1 The fit procedure

The mathematical formalism of the fit procedure can be found in reference [13]. The tagging algorithm classified the $N_F = 3$ flavours of the hadronic events into $N_T = 6$ categories. The first set of observables was the matrix $D_{IJ}, (I, J = 1, ..., N_T)$ defined as the fraction of events tagged as $I$ and $J$ for hemispheres 1 and 2 respectively. The expected fraction of events $T_{IJ}$ can be written as

[2] An additional smearing including the simulated and data statistical errors was applied on the weighting procedure.

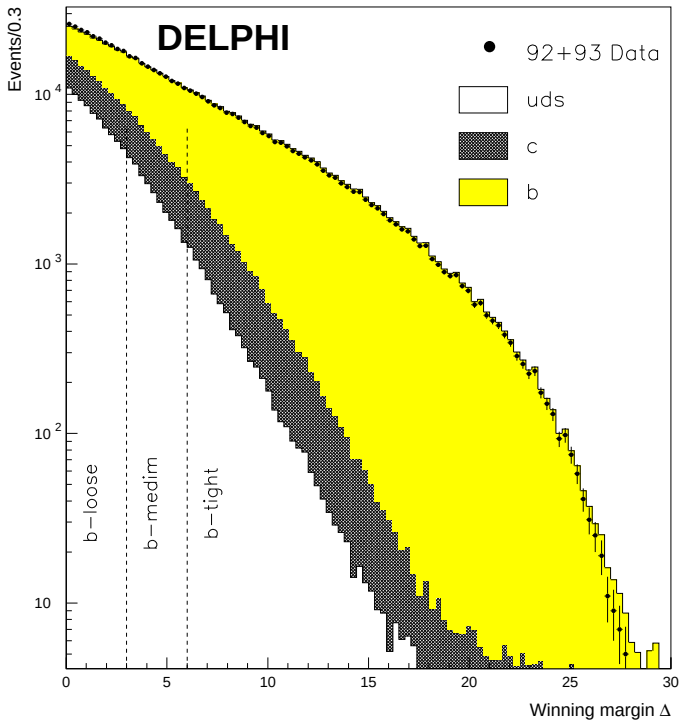


Figure 6: Winning margin $\Delta$ distributions in the $b$ tag for data and simulation after correction. Each filled area style shows the different flavour contributions to the events in a given tag obtained from simulation. The values of the cuts defining the categories are also indicated. Simulation distributions were normalized to the data statistics.

$$T_{IJ} = \sum_l C_I^l C_J^l (1 + \rho_{JI}^l) R_l \tag{8}$$

In equation (8), $R_l$ is the flavour fraction for a given sample ($R_b = \Gamma_{b\bar{b}}/\Gamma_{had}$ is the resultant required branching ratio). $C_I^l$ is the probability to classify an hemisphere of flavour $l$ into the category $I$. The $6 \times 3$ array $C_I^l$ (called *classification matrix*) was assumed to be the same for both hemispheres. In a first approximation, the probability to classify an event of a given flavour $l$ in one hemisphere is independent of the classification in the other hemisphere. In order to take into account inter-hemisphere correlations the correlation matrix $\rho_{JI}^l$ was introduced. If the hemispheres are independent, all $\rho_{JI}^l$ elements are equal to zero. The values of these elements estimated from simulation can be found in [14]. Most of them are small or not significant.

It is not possible to extract $R_b$ by a simple fit of the matrix $D_{IJ}$ because of the rotation degeneracy described in [13]. To solve this problem, a second set of observables, the distributions of the category fractions $f_I(\Delta)$, were used in the fit. In the sample of events which were tagged as $b$ in one hemisphere with a winning margin $\Delta$, $f_I(\Delta)$ is defined as the fraction of events classified in the category $I$ for the other hemisphere. The main property of this ratio is that its asymptotic value provides an estimation of the $C_I^b$ column of the classification matrix [14].

Using both sets of observables (the matrix $D_{IJ}$ and the distributions $f_I(\Delta)$) the mini-

mization of the global objective $\chi^2(C, R)$ function defined in [14] allows us the simultaneous determination of the classification matrix and the $R_l$ compositions. With this function a remaining degeneracy in the $uds - c$ sector is still present but it can be removed, for instance, by fixing $R_c$ to the Standard Model value. This constraint has no effect on any parameter of the $b$ sector. As in this analysis the $uds$ and $c$ sectors are decoupled from the $b$ sector and the corresponding background efficiencies in $b$ categories are small; the double tag correlation coefficients for $uds$ flavour have a small enough influence on $R_b$ and thus are not included in the minimization of $\chi^2(C, R)$.

## 6.2 $\Gamma_{b\bar{b}}/\Gamma_{had}$ measurement and consistency checks

The data samples collected in 1992 and 1993 were analyzed independently because differences in the microvertex detector was expected to result in slightly different tagging efficiencies. The plots of the $f_I(\Delta)$ distributions as a function of the clear winning cut value $\Delta$ are shown in figure 7 for the DELPHI 1992/1993 data. The reproducibility and reliability of the method was controlled by analyzing the same Monte Carlo events that were also used in the estimation of the correlation coefficients. The Monte Carlo $f_I(\Delta)$ distributions are also shown in figure 7 together the contributions of $uds$, $c$ and $b$ flavours. No significant irreducible $uds$ and $c$ background is observed in the asymptotic region, especially in the $f_4(\Delta)$, $f_5(\Delta)$ and $f_6(\Delta)$ distributions which are the most significant for the $R_b$ extraction. Effects of remaining background are small and are included in the systematic uncertainties.

In the fit of the $\chi^2(C, R)$ function, the $R_c$ parameter was fixed to the Standard Model value of 0.171. Even though there were a large number of free parameters in the fit, no local minima were seen in the whole range of $R_b$ [14]. Table 7 summarizes for simulation and real data the fitted $C_I^b$ and $R_b$ values obtained taking into account efficiency correlations. A comparison with the expected values for simulation is also given in table 7. The $C_1^b$ element is the least well reproduced. Background effects were not negligible in this $b$ depleted category and $2\sigma$ differences were observed. However this matrix element was not significant in the $R_b$ extraction. For all the other extracted $C_I^b$ parameters, $C_I^{uds}$ and $C_I^c$, good agreement was found between the sets of expected and fitted values.

Table 7 shows that the difference between the generated and the fitted $R_b$ is $0.0018 \pm 0.0027$ in 1992 and $-0.0007 \pm 0.0026$ in 1993. Therefore, on average the measured values agree within $0.0005 \pm 0.0018$ with the expected ones so it may be concluded that the method produces no bias on the measurement.

In 1993 DELPHI took data at three different centre-of-mass energies, $E_{CMS}$, around the $Z$ peak (91.2 GeV). Of the total of 487673 events, 56194 were selected at $E_{CMS}$=89.45 GeV, 344655 at $E_{CMS}$=91.2 GeV and 86824 at $E_{CMS}$=93.04 GeV. The off-peak data are expected to have almost the same fraction of $b\bar{b}$ events as the hadronic cross-sections at these energies are still dominated by the $Z$ exchange. Therefore the off-peak data can be analyzed together with the 1993 on-peak data. However, from analyses of the three subsets independently, the results of the fits were $R_b = 0.2218 \pm 0.0157$ for $E_{CMS}$=89.45 GeV, $R_b = 0.2208 \pm 0.0059$ for $E_{CMS}$=91.2 GeV and $R_b = 0.2184 \pm 0.0139$ for $E_{CMS}$=93.04 GeV. The corresponding probabilities of the fits were 45.3 %, 74.5 % and 37.6 % respectively. As the difference between the value of $R_b$ for different energies of the beams and its value at the $Z$ peak (91.2 GeV) is not sensitive to systematic effects these numbers can be combined using only statistical errors. Before the average, the off-peak values of $R_b$ were

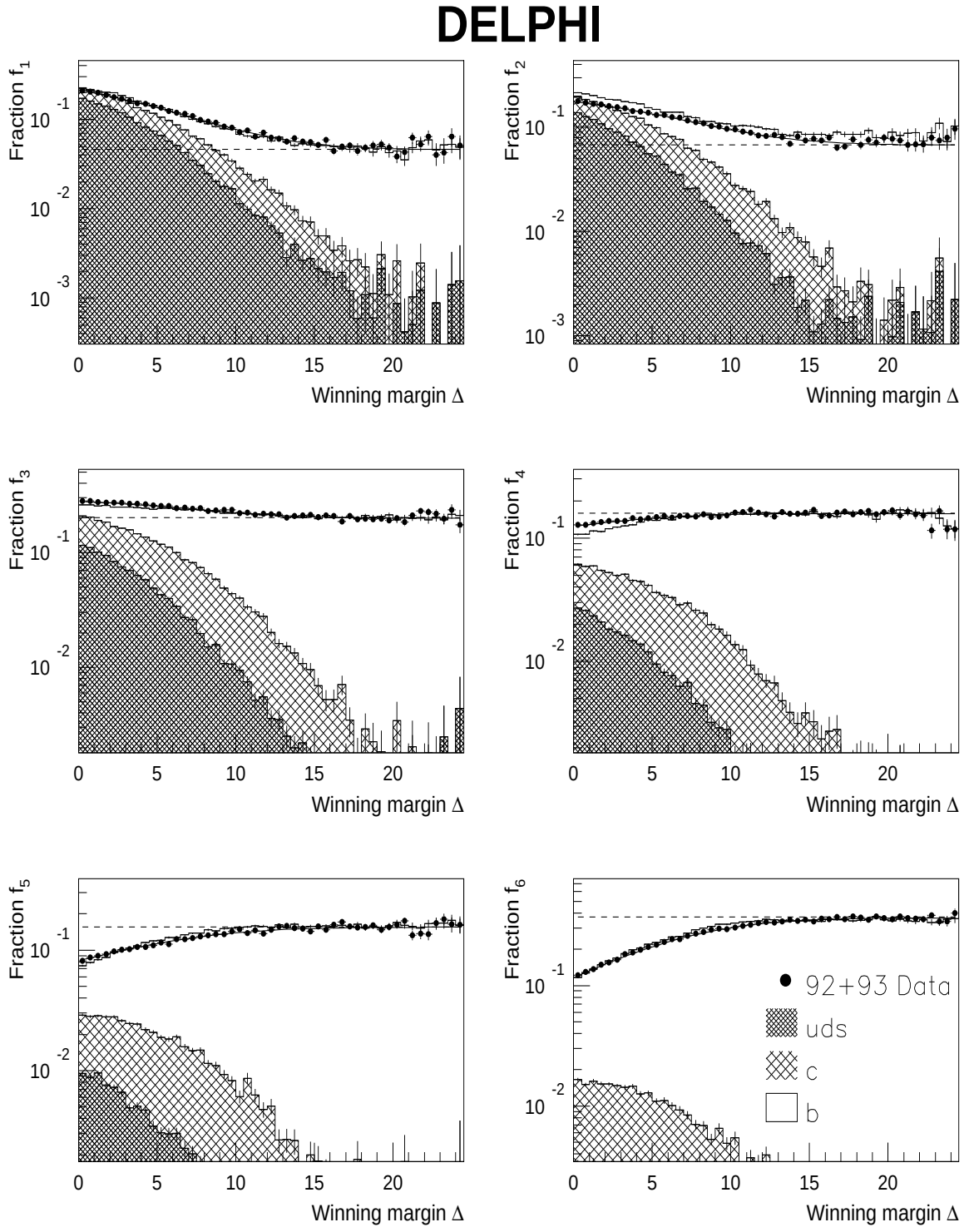


Figure 7: $f_I(\Delta)$ distributions with their asymptotic fits for all the data. The dotted horizontal lines show the fitted $C_I^b$ values for the data. The distributions estimated from simulation are also shown together with the contributions of $uds$, $c$ and $b$ flavours.

| Parameter | 1992 Simulation | | 1992 Data | 1993 Simulation | | 1993 Data |
|---|---|---|---|---|---|---|
| | *Expected* | *Fitted* | *Fitted* | *Expected* | *Fitted* | *Fitted* |
| $C_1^b$ | 0.0507 | 0.0523(10) | 0.0568(20) | 0.0500 | 0.0517(09) | 0.0357(18) |
| $C_2^b$ | 0.0731 | 0.0732(09) | 0.0802(15) | 0.0659 | 0.0665(07) | 0.0600(18) |
| $C_3^b$ | 0.1974 | 0.1971(15) | 0.2041(26) | 0.1985 | 0.1976(14) | 0.1821(21) |
| $C_4^b$ | 0.1458 | 0.1458(09) | 0.1537(16) | 0.1473 | 0.1470(08) | 0.1580(10) |
| $C_5^b$ | 0.1435 | 0.1430(08) | 0.1478(14) | 0.1449 | 0.1442(07) | 0.1618(15) |
| $C_6^b$ | 0.3895 | 0.3885(18) | 0.3575(35) | 0.3935 | 0.3931(17) | 0.4025(34) |
| $R_b$ | 0.217 | 0.2188(27) | 0.2148(51) | 0.217 | 0.2163(26) | 0.2206(51) |
| $Prob(\chi^2)$ | | 9.5% | 22.0% | | 81.7% | 10.9% |

Table 7: Results of the DELPHI 1992/1993 simulation and real data fits with the correlation pattern taken from Monte Carlo. Comparison with the expected values for simulation. Statistical errors are also given in brackets and affect the last two digits.

corrected by the small changes with respect to the on-peak value. These corrections were predicted by ZFITTER [19] and reduced the off-peak value with respect to the on-peak one by 0.0007 and 0.0005 for $E_{CMS}$=89.45 GeV and $E_{CMS}$=93.05 GeV respectively. The values for 1993 in table 7 show the results of combining the three energies after these corrections. This result agrees at the level of three per mil with the result obtained when all the statistics are analyzed together, which is a consistency check of the reproducibility and reliability of the method. However, it should be noted that, owing to small changes in efficiencies for the different energies of the colliding beams, the probability of the fit for the overall statistics is smaller than for each data subset.

As a cross check on the effect of correlations, we have repeated the same fits of table 7 taking all correlation coefficients equal to zero. Table 8 summarizes the differences between the results of the fit when correlations are considered and when they are taken equal to zero for the real data samples. The smallness of the change in the results is remarkable. So, for $R_b$ the change is at the level of 0.5 % of the measurement and has different sign for 1992 and 1993 data, which can be explained as a statistical effect on the estimates of the correlations. This is a evidence that the sensitivity of the method to the provided pattern of correlations is small. For the simulated samples similar results were obtained.

| Parameter | 1992 Data | 1993 Data |
|---|---|---|
| $C_1^b$ | $+0.00043 \pm 0.00058$ | $+0.00044 \pm 0.00045$ |
| $C_2^b$ | $+0.00154 \pm 0.00044$ | $-0.00061 \pm 0.00038$ |
| $C_3^b$ | $+0.00026 \pm 0.00085$ | $+0.00094 \pm 0.00078$ |
| $C_4^b$ | $-0.00093 \pm 0.00048$ | $+0.00065 \pm 0.00042$ |
| $C_5^b$ | $-0.00119 \pm 0.00051$ | $-0.00090 \pm 0.00050$ |
| $C_6^b$ | $-0.00012 \pm 0.00102$ | $-0.00052 \pm 0.00084$ |
| $R_b$ | $+0.00103 \pm 0.00161$ | $-0.00146 \pm 0.00150$ |

Table 8: Differences between the results of the fit when correlations are considered and when they are taken equal to zero for DELPHI 1992/1993 real data samples. Errors include only uncertainties on correlations coming from the limited simulation statistics. Similar results are obtained for the simulated data samples.

## 6.3 Systematic errors

The three kinds of systematic errors were studied separately: uncertainties coming from model uncertainties, detector effects and finally uncertainties from the analysis method.

### 6.3.1 Model uncertainties

Most methods of extraction of the $R_b$ quantity assume the knowledge of the tag efficiencies or contaminations for the $uds$ and $c$ flavours [3, 15, 16]. These quantities, taken from simulation, are sensitive to theoretical uncertainties in the $uds$ and $c$ sectors and are sources of systematic error. This is not the case in this method. $R_b$ is extracted simultaneously with the efficiencies/contaminations by fitting the data. However, the analysis assumes that asymptotically the contributions of $uds$ and $c$ are negligible.

In the absence of hemisphere correlations and remaining $uds$ and $c$ background in the region of hard cuts, the $R_b$ measurement is mathematically independent of the factors that affect $b$ production or decays, for example fragmentation or lifetimes. Then the corresponding systematic errors are exactly zero. If the hypothesis is almost true, second order effects on the $R_b$ measurement can appear and should be included in the systematic uncertainties.

In the previous section it was shown that a small difference in $R_b$ is observed if the estimated correlation matrix is taken into account in the fit or if it is neglected. This small bias suggests that the method is insensitive to the particular pattern of correlations. There is no evidence for a fundamentally different correlation pattern in real data compared to the simulation. The error made on data coming from correlations should be similar to the one made on the simulation. An estimate of this error was obtained by varying the parameters of the simulation which could be sources of correlation.

By following the prescriptions described in reference [9], we have checked that errors due to modeling are of second order. Table 10 summarizes all the contributions to the systematic error coming from model uncertainties.

Correlation effects can be described in terms of the following sources [9]:

- Hadronic $Z$ events with three or more jets differ from those with a two jet topology by the presence of one or more hard gluons in the final state, which might be a source of negative correlation in the double $b$ tag. This effect includes the hard gluon emission producing a $b\bar{b}$ pair in the same hemisphere (about 2 % of the $b\bar{b}$ events according to the simulation). To obtain the systematic error from this source, the number of events was measured in data and in simulation as a function of the thrust of the event. Then, the simulation distribution was corrected to reproduce the corresponding data distribution. The error was estimated as the change in the fitted value of $R_b$ due to the change of correlations between the standard simulation and the corrected one. The quoted value was 0.00057.

- The bias of the production vertex due to the inclusion of tracks from $b$ decays can produce a negative correlation. The lifetime of B hadrons and the $b$ fragmentation function are the best parameters to describe this effect. The change of correlations from a variation of the $b$ lifetime was estimated by using the same simulated sample with different weightings. The $b$ lifetime was varied within the error of [9]. The change in correlations leads to a variation on $R_b$ of 0.00022. The uncertainty due

to the $b$ fragmentation function was estimated similarly by varying the Peterson parameter to reproduce the mean energy of B hadrons within the error limits of [9]. The resultant error was 0.00038.

- Finally, the uncertainties in the correlations coming from the limited simulation statistics shown in table 8 must be included.

For the evaluation of the systematic uncertainty coming from remaining $uds$ and $c$ background the following contributions were considered [9]:

- The error on $R_b$ due to actual amount of charm events (which should be distinguished from the formal $R_c$ parameter of the fit) was estimated changing the $c\bar{c}$ fraction by 8% around its measured value ($R_c = 0.171 \pm 0.014$. A contribution to the systematic error of $\mp 0.00040$ was found. Moreover, the $R_c$ parameter was varied in the same interval and the change of $R_b$ was exactly zero.

- The uncertainty due to the $c$ fragmentation function was estimated by varying the Peterson parameter to reproduce the mean energy of D hadrons within the error limits of [9].

- The uncertainties from the relative production rate of D hadrons, their lifetimes, decay multiplicities and inclusive branching ratios $D \to K^0 X$ were obtained by varying their measured values according to [9].

- The systematic error from uncertainties in the production of long lived particles in light quark events ($K^0$, $\Lambda$, hyperons) was obtained by varying the corresponding production rates in the simulation by $\pm 10\%$.

- The systematics from the gluon splitting $g \to b\bar{b}$ and $g \to c\bar{c}$ was obtained from the variation of fraction of such events by 50 % as proposed in [9].

To obtain the systematic error from these sources, the Monte Carlo events were weighted as a function of the model parameter. The weighted simulated sample was fitted and the result compared with the expected one. The difference with respect to the standard simulated sample was taken as the error.

### 6.3.2 Detector effects

The detector effects include all sources of uncertainties due to apparatus and can be described in the following terms:

- Detector response. Differences between data and Monte Carlo are not important in the present analysis because all efficiencies and backgrounds are obtained directly from the data and only a small remaining model dependence appears due to efficiency correlation effects and eventual remaining background in the region of hard cuts. The Monte Carlo sample was corrected to adjust the winning margin distribution to the data. This procedure improves the agreement between data and simulation at the level of the $D_{IJ}$ matrix and the $f_I(\Delta)$ distributions. As the analysis is the same in both simulated samples an estimate of the uncertainty due to the knowledge of the detector response was obtained as the difference between the

measurements using the standard simulated sample and the corrected one plus the error on this difference. The values obtained were 0.00038 for the 1992 sample and 0.00089 for 1993.

- The polar angle of the thrust axis. Correlation effects could be induced due to the drop of tag efficiency at the fringes of the vertex detector acceptance since both jets either are in a region of good or somewhat worse VD acceptance. To obtain the systematic error from this source the number of $b$ tagged events was measured in data and in simulation as a function of $\mid cos\theta_{thrust} \mid$. The simulation distribution was corrected in order to reproduce the corresponding data distribution. For the error, we take the difference between the measurements using the standard simulation and the corrected one and we add in quadrature the error on this difference. We find a contribution of 0.00042 for 1992 and 0.00041 for 1993.

- The azimuthal angle of the jets. Due to dead or noisy modules in the vertex detector the efficiency was not flat in the azimuthal angle. In particular, during the 1992 running, one row of the DELPHI vertex detector in one layer was dead. In an almost back to back jet topology a bad module hit on one side results normally in a good module hit in the other side, producing a negative correlation. The multidimensional tagging is not sensitive to local defects, so the variation of the tag efficiency with the azimuthal direction of the event axis is not important. Nevertheless, we have investigated the error due to the local drop of efficiency which induces a small negative correlation. The method used was the same as for the polar angle correlation and a contribution of 0.00034 for 1992 and 0.00009 for 1993 was found.

- Beam spot constraint. This constraint can be a source of correlations owing to the beam spot size, since the beam spot constraint is common for both hemispheres. A 10% uncertainty was assumed (which corresponds to the accuracy of the size determination) and a variation on $R_b$ of 0.00034 was found for both the 1992 and 1993 years.

- Acceptance bias. The bias of $Z \rightarrow b\bar{b}$ fraction in the final sample was estimated from simulation and was found small, $(0.23 \pm 0.20)$ % for 1992 in relative value and $(0.42 \pm 0.17)$ % for 1993. That induces a systematic uncertainty on $R_b$ of 0.00043 for 1992 and 0.00037 for 1993.

### 6.3.3 Uncertainties specific to the method

The fit to the simulation performed in section 6.2 shows that the analysis method works within the accuracy given by the Monte Carlo statistical precision. In particular, it was shown that the difference between the generated and the fitted $R_b$ is $0.0018 \pm 0.0027$ in 1992 and $-0.0007 \pm 0.0026$ in 1993. By other hand, as was indicated in section 6.1, the method assumes that estimations of the $C_I^b$ column of the classification matrix can be extracted asymptotically. The effect of this assumption can be tested by fitting $R_b$ in the simulation with the $C_I^b$ parameters fixed to their true values. The difference obtained with respect to the full measurement was $0.0011 \pm 0.0022$ for 1992 and $-0.0001 \pm 0.0021$ for 1993, where errors are the statistical differences of both measurements. These values were used to correct the $R_b$ derived from the fits to the data and theirs errors were taken as a systematic uncertainty on the measurement which considers effects from the analysis

| | 91 Data | 92 Data | 93 Data | Combined |
|---|---|---|---|---|
| Result | 0.22410 | 0.21372 | 0.22074 | 0.21863 |
| Statistical error | $\pm$0.00630 | $\pm$0.00509 | $\pm$0.00510 | $\pm$0.00318 |
| Model uncertainties | | | | $\pm$0.00077 |
| Simulation statistics on correlations | $\pm$0.00277 | $\pm$0.00161 | $\pm$0.00150 | $\pm$0.00104 |
| $c\bar{c}$ events ($\Gamma_{c\bar{c}}/\Gamma_{had}$) | | | | $\pm$0.00040 |
| Detector response | $\pm$0.00087 | $\pm$0.00038 | $\pm$0.00089 | $\pm$0.00068 |
| Polar angle acceptance | $\pm$0.00075 | $\pm$0.00042 | $\pm$0.00041 | $\pm$0.00048 |
| Azimuthal angle acceptance | $\pm$0.00093 | $\pm$0.00034 | $\pm$0.00009 | $\pm$0.00036 |
| Beam spot size | | | | $\pm$0.00034 |
| Acceptance bias | $\pm$0.00070 | $\pm$0.00043 | $\pm$0.00037 | $\pm$0.00027 |
| Analysis method | $\pm$0.00384 | $\pm$0.00222 | $\pm$0.00210 | $\pm$0.00145 |
| Total systematic error | $\pm$0.00509 | $\pm$0.00300 | $\pm$0.00295 | $\pm$0.00221 |
| Total error | $\pm$0.00810 | $\pm$0.00591 | $\pm$0.00589 | $\pm$0.00388 |

Table 9: Breakdown of the error and the combination of results of $\Gamma_{b\bar{b}}/\Gamma_{had}$ obtained from the multivariate tag for each year and the obtained one from the combination. Common systematic errors are only written in the column of the combined analysis.

method. This becomes the most important contribution to the systematic error which is uncorrelated between the different years and could be reduced with more simulation statistics.

Therefore we quote as final values, including acceptance and systematic corrections

$$R_b = 0.2137 \pm 0.0051(stat) \pm 0.0030(syst)$$

and

$$R_b = 0.2207 \pm 0.0051(stat) \pm 0.0030(syst)$$

for 1992 and 1993 data respectively.

## 6.4 Combination of the 91 to 93 results

In order to combine the analyses presented here with the corresponding one made with the 1991 data, the following assumptions are made:

- All statistical errors are assumed to be independent.
- The errors due to model uncertainties on efficiency correlations and $b$ tag backgrounds are taken fully correlated.
- The error due to $\Gamma_{c\bar{c}}/\Gamma_{had}$ was assumed to be fully correlated.
- The error from acceptance bias was assumed uncorrelated.
- All other errors from detector effects are zero for the 1991 analysis because they were assumed to be well described within the statistical error from the fit to the simulation. In order to be consistent in the average, for this year these errors have been recomputed using the same method described previously. Finally they were conservatively assumed to be fully correlated.

With these assumptions the final result is

$$R_b = 0.2186 \pm 0.0032(stat) \pm 0.0022(syst) \pm 0.0004(\Gamma_{c\bar{c}}) \quad (9)$$

The values from the off-peak data taken in 1993 have been corrected for the small expected change to the on-peak value as explained in section 6.2 the off-peak 1991 data, being of much smaller significance, have not been corrected.

The breakdown of the error and the combination of results are given in table 9.

# 7 Combination of the Results

The results from the different analyses have been combined taking into account the common systematic errors. The statistical correlation between the mixed tag and the other analyses can be neglected. The correlation between the double vertex tag and the multivariate analysis has been estimated using a Monte Carlo technique to be less than 0.35 (90% C.L.). Conservatively this value has been used in the average[3]. The combined result is:

$$R_b = 0.2210 \pm 0.0016(stat) \pm 0.0020(syst) \pm 0.0012(R_c).$$

The breakdown of the error is given in table 10.

# 8 Conclusions

Three different measurements of the partial decay width $R_b$ of the $Z$ into $b$-hadrons have been performed. Events were selected either by leptons carrying high transverse momentum or with tracks having a large impact parameter. From the different analyses the following results were obtained:
Double lifetime tag:

$$R_b = 0.2216 \pm 0.0017(stat) \pm 0.0027(syst) \pm 0.0018(R_c)$$

Mixed tag:

$$R_b = 0.2231 \pm 0.0029(stat) \pm 0.0035(syst) \pm 0.0012(R_c)$$

Multivariate analysis:

$$R_b = 0.2186 \pm 0.0032(stat) \pm 0.0022(syst) \pm 0.0004(R_c).$$

The $R_c$ error always corresponds to a $R_c$ variation of 8% around its Standard Model value.

Combining all numbers the following result is obtained:

$$R_b = 0.2210 \pm 0.0016(stat) \pm 0.0020(syst) \pm 0.0012(R_c).$$

All results are in agreement with those of other measurements at LEP [15, 16]. Assuming a mass of the top quark of $m_t = 180 \pm 12$ GeV as obtained from a simple average of the CDF [17] and the D0 [18] measurements the Standard Model predicts $R_b = 0.2155 \mp 0.0005$

[3]The most probable value for the correlation was found to be 0. It has been checked the final result doesn't change using this value.

| Error Source | Range | Uncertainty dvt | mt | mult | comb. |
|---|---|---|---|---|---|
| Internal experimental effects: | | | | | |
| Hemisphere correlations | | $\pm 0.0011$ | 0 | $\pm 0.00144$ | $\pm 0.0008$ |
| Lepton-vertex correlations | | 0 | $\pm 0.0013$ | 0 | $\pm 0.0003$ |
| Resolution function | | $\pm 0.0009$ | $\pm 0.0009$ | $\pm 0.00068$ | $\pm 0.0008$ |
| Lepton sample purity | | 0 | $\pm 0.0019$ | 0 | $\pm 0.0004$ |
| acceptance bias | | $\pm 0.0002$ | 0 | $\pm 0.00027$ | $\pm 0.0001$ |
| Method | | 0 | 0 | $\pm 0.00145$ | $\pm 0.0005$ |
| $\langle x_E(c) \rangle$ | $0.49 \pm 0.02$ | $\mp 0.0005$ | $\mp 0.0005$ | $\pm 0.00015$ | $\mp 0.0004$ |
| $\mathrm{Br}(c \to \ell)$ | $(9.8 \pm 0.5)\%$ | 0 | $\pm 0.0010$ | 0 | $\pm 0.0002$ |
| Semilept. model $b \to \ell$ [9] | $(^{+\mathrm{ACCMM}}_{-\mathrm{ISGW**}})$ | 0 | $\pm 0.0011$ | 0 | $\pm 0.0002$ |
| Semilept. model $c \to \ell$ [9] | ACCMM1 $(^{+\mathrm{ACCMM2}}_{-\mathrm{ACCMM3}})$ | 0 | $\mp 0.0008$ | 0 | $\mp 0.0002$ |
| $D^0$ fraction in $c\bar{c}$ events | $0.557 \pm 0.053$ | $\mp 0.0001$ | $\mp 0.0001$ | $\mp 0.00002$ | $\mp 0.0001$ |
| $D^+$ fraction in $c\bar{c}$ events | $0.248 \pm 0.037$ | $\mp 0.0013$ | $\mp 0.0008$ | $\mp 0.00005$ | $\mp 0.0008$ |
| $(D^0 + D^+)$ fraction in $c\bar{c}$ events | $0.80 \pm 0.07$ | $\mp 0.0008$ | $\mp 0.0005$ | $\mp 0.00006$ | $\mp 0.0005$ |
| $D_s$ fraction in $c\bar{c}$ events | $0.15 \pm 0.03$ | $\mp 0.0006$ | $\mp 0.0004$ | $\mp 0.00022$ | $\mp 0.0004$ |
| $D^0$ lifetime | $0.420 \pm 0.008$ ps | $\mp 0.0003$ | $\mp 0.0002$ | $\mp 0.00004$ | $\mp 0.0002$ |
| $D^+$ lifetime | $1.066 \pm 0.023$ ps | $\mp 0.0004$ | $\mp 0.0002$ | $\mp 0.00003$ | $\mp 0.0002$ |
| $D_s$ lifetime | $0.450^{+0.030}_{-0.026}$ ps | $\mp 0.0003$ | $\mp 0.0002$ | $\mp 0.00004$ | $\mp 0.0002$ |
| $\Lambda_c$ lifetime | $0.191^{+0.015}_{-0.012}$ ps | 0 | 0 | $\mp 0.00007$ | 0 |
| D decay multiplicity | $2.53 \pm 0.06$ | $\mp 0.0006$ | $\mp 0.0004$ | $\mp 0.00002$ | $\mp 0.0004$ |
| $BR(D \to K^0 X)$ | $0.46 \pm 0.06$ | $\pm 0.0008$ | $\pm 0.0007$ | $\pm 0.00005$ | $\pm 0.0006$ |
| g $\to b\bar{b}$ per multihadron | $(0.18 \pm 0.09)\%$ | $\mp 0.0003$ | $\mp 0.0003$ | $\mp 0.00001$ | $\mp 0.0002$ |
| g $\to c\bar{c}$ per multihadron | $(1.3 \pm 0.7)\%$ | $\mp 0.0001$ | $\mp 0.0001$ | $\mp 0.00001$ | $\mp 0.0001$ |
| Rate of long-lived light hadrons | Tuned JETSET$\pm$10% | $\mp 0.0006$ | $\mp 0.0005$ | $\mp 0.00004$ | $\mp 0.0004$ |
| $R_c$ | $0.171 \pm 0.0014$ | $\mp 0.0018$ | $\mp 0.0012$ | $\mp 0.00040$ | $\mp 0.0012$ |

Table 10: Summary of systematic errors on $R_b$ obtained from the double vertex tag (dvt, section 4), the mixed tag (mt, section 5), the multivariate tag (mult, section 6) and the combination of the three analyses. Detailed explanations how the different error sources are obtained can be found in [9].

[19] whereas $R_c$ does not depend significantly on other parameters. This number is about 2.1 standard deviations lower than our measurement assuming $R_c = 0.171$.

In addition the ratio of the fraction of $b\bar{b}$-events in the hadronic event sample between the peak and the off peak energies has been measured. The values

$$\frac{R_b(89.49GeV)}{R_b(91.25GeV)} = 0.982 \pm 0.015$$
$$\frac{R_b(93.08GeV)}{R_b(91.25GeV)} = 0.997 \pm 0.016$$

have been found, well in agreement with the standard model prediction of 0.997 and 0.998.

## Acknowledgements

We are greatly indebted to our technical collaborators and to the funding agencies for their support in building and operating the DELPHI detector, and to the members of the CERN-SL Division for the excellent performance of the LEP collider.

# References


[1] See, for example,
J.H. Kühn, P.M. Zerwas, in: *Z Physics at LEP 1*, eds. G. Altarelli, R. Kleiss and C. Verzegnassi, Vol. 1 (CERN 89-08, 1989) pp. 271-275.

[2] DELPHI Collab., *DELPHI Results on Electroweak Physics with Quarks*, DELPHI 94-111 PHYS 428, Contributed to the Glasgow Conference, and references therein.

[3] P.Abreu *et al.* (DELPHI Collaboration), Z. Phys. **C66** (1995) 323.

[4] P.Abreu *et al.* (DELPHI Collaboration), Z. Phys. **C65** (1995) 555.

[5] DELPHI Collaboration, P. Aarnio et al., Nucl. Inst. Meth. **A303** (1991) 233.

[6] N. Bingefors et al., Nucl. Inst. Meth. **A328** (1993) 447.

[7] T. Sjöstrand et al., in *"Z physics at LEP 1"*, CERN 89-08, CERN, Geneva, 1989. Comp. Phys. Comm. **39** (1986) 347.

[8] DELSIM Reference Manual, DELPHI 87-98 PROG 100, Geneva, 1989.

[9] The LEP Electroweak Working Group, ALEPH Note 94-30, DELPHI 94-23 Phys 357, L3 Note 1577, OPAL Technical Note TN213 , 28 February, 1994;
The LEP Electroweak Working Group, ALEPH note 94-90, DELPHI 94-23 Phys 357/add, L3 Note 1613, OPAL Technical Note TN237 , 10 June, 1994 .

[10] D. Coffman et al., (MARK III Collaboration), Phys.Lett. **B263** (1991) 135.

[11] Particle Data Group - Review of Particle Properties - Phys. Rev. **D45** (1992) 1.

[12] F. Caravaglios, G. Ross, Phys. Lett. **B346** (1995) 159.

[13] P. Billoir *et al.*, CERN-PPE/94-189 to be published in NIM

[14] F. Martinez-Vidal *et al.*, DELPHI 95-85 PHYS 520.

[15] ALEPH Collaboration, D. Buskulic et al., Phys. Lett. **B313** (1993) 535.

[16] OPAL Collaboration, P.D. Acton et al., Z. Phys. **C65** (1995) 17.

[17] CDF Collaboration, F. Abe et al., *Observation of Top Quark Production in $p\bar{p}$ collisions*, FERMILAB-PUB-95/022-E.

[18] DØ Collaboration, S. Abachi et al., *Observation of the Top Quark*, FERMILAB-PUB-95/028-E.

[19] D. Bardine et al., *ZFITTER: An Analytical Program for Fermion Pair Production in $e^+e^-$ Annihilation*, CERN-TH 6443/92 (May 1992).